Electrical Power and Energy Systems 99 (2018) 630–637

Contents lists available at ScienceDirect

Electrical Power and Energy Systems

journal homepage: www.elsevier.com/locate/ijepes

Review

The transient-state effect of the reactive power control of photovoltaic systems on a distribution network

Insu Kim[a,*], Ronald G. Harley[b,c]

[a] Department of Electrical Engineering, Inha University, Incheon, 22212, South Korea
[b] Electrical and Computer Engineering, Georgia Institute of Technology, Atlanta, GA 30332 USA
[c] Professor Emeritus at the University of KwaZulu-Natal, Durban, South Africa

ARTICLE INFO

Keywords:
DIgSILENT
OpenDSS
Photovoltaic (PV) systems
Reactive power control
Transient-state response
Volt/Var control

ABSTRACT

Despite of their small capacity, distributed generation (DG) systems can cause an increase in feeder voltage when they produce power into a distribution system if not appropriately controlled. To prevent such an increase in voltage, the state-of-the-art inverter can adjust reactive power, referred to as Volt/Var control. Furthermore, such an inverter-based DG system has been continuously connected to a large distribution network. Thus, the objective of this study is to present an optimal reactive power control method for DG systems, particularly photovoltaic (PV) systems, in the steady state. The second objective of this study is to analyze the transient-state response of a sufficiently large distribution network integrated by high-capacity PV systems able to control reactive power. The large network can be more efficiently developed by a steady-state power-flow analysis program, or OpenDSS based on text editors, than a transient-state analysis program based on graphical editors. Therefore, this study proposes a method that imports the feeder models developed in OpenDSS into a transient-state power systems analysis program, or DIgSILENT. That is, the proposed method models a sufficiently large actual distribution network with thousands of nodes and high-capacity PV systems able to control reactive power. Then, this study examines transient-state dynamics of the feeders. From the steady- and transient-state analyses, this study found that high-capacity PV systems with the capability of Volt/Var control could mitigate an increase in voltage caused by their power injection to the feeder and they could regulate the voltage of a bus to which they are connected within a set voltage range if they are optimally controlled.

1. Introduction

To reduce the energy dependence on the conventional generators, various distributed generation (DG) systems have been connected to a distribution network. When they produce power, they can increase feeder voltage because of their reverse power flow, if they are not appropriately controlled. Therefore, during the last a few decades, many researchers have examined the transient-state response of a distribution network that hosts such a DG system [2]. For example, some studies solved electromagnetic transient-state problems of a distribution network [3,4]. Furthermore, available simulation methods and tools for transient-state analyses were overviewed in [5]. Since these studies did not present the detailed modeling of a specific power system component, one study proposed an analytical method for the transient-state analysis of induction motor, lighting, and resistor loads by their power balance equations [6]. Another study presented a detailed model of photovoltaic (PV) and wind systems [7]. Using Power Systems Computer Aided Design (PSCAD), the transient-state model of a grid-connected microturbine system was presented in [8]. Grid-connected inverters were also modeled in [9,10].

While the previous studies have modeled various power systems components for transient-state analyses, they did not compare simulation results to actual measurement. Thus, after comparing simulation results to actual measurement values, one study claimed that short-circuit studies simulated in the transient state could provide an accurate understanding of feeder dynamics [11,12].

Meanwhile, since the previous studies did not examine the transient-state response of a distribution network that hosts DG systems, several studies simulated a distribution network integrated by DG systems such as wind, solar PV, hydropower, gas turbines, diesel engines, and induction generators [13–20]. For example, a distribution network that hosts a hybrid DG system such as a wind turbine, PV, and hydro power was analyzed by Digital Simulation and Electrical Network Calculation Program (DIgSILENT) [13]. The transient-state behaviors of a small test feeder were analyzed by the nonlinear models of gas, diesel turbine, and excitation systems implemented in Simulink of MATLAB

* Corresponding author.
E-mail address: su@inha.ac.kr (I. Kim).

https://doi.org/10.1016/j.ijepes.2018.01.015
Received 12 July 2017; Received in revised form 9 December 2017; Accepted 11 January 2018

Nomenclature

DC	direct current
DG	distributed generation
D_i	the droop value of photovoltaic (PV) system i in percent
$\Delta I_{q,i,a}^{(k)}$	the current injected to phase a of bus i at the kth iteration
$\delta_{V,i,a}^{(k)}$	the voltage angle of phase a of bus i at the kth iteration
ΔV_i	the deviation from the setting voltage of bus i or a bus to which PV system i is connected
MPPT	maximum power point tracking
OLTC	on-load tap changing
pf_i	the power factor limit of bus i (e.g., either leading or lagging 0.9 or higher [1])
PI	proportional integral (controller)
PV	photovoltaic
PF	power factor
$P_{min,i}$ and $P_{max,i}$	the minimum and maximum active power of PV system i, respectively
$P_{PV,i}^{(k)}$ and $Q_{PV,i}^{(k)}$	the active and reactive power output of PV system i at the kth iteration
Q_i	the reactive power generation output of PV system i
$Q_{min,i}$ and $Q_{max,i}$	the minimum and maximum reactive power of PV system i, respectively
$Q_{setpoint,i}$	the set value of the reactive power output of PV system i
Sign (ΔV)	$+1$ if $\Delta V > 0$, otherwise -1
$S_{nom,i}$	the nominal power of PV system i
SVC	static var compensator
V_i	the terminal voltage of a bus to which PV system i is connected
$V_{pos,i}^{(k)}$	the positive-sequence voltage of bus i at the kth iteration
$V_{setpoint,i}$	the positive-sequence setting voltage of a bus to which PV system i is connected
$Z_{bus,i}$	the ith diagonal element of the positive-sequence impedance matrix

[14]. The transient-state impact of a fault event on the actual distribution system with synchronous generators designed in Simulink of MATLAB was examined in [15]. Recently, one study investigated the transient-state response of a 10 kV distribution system with induction, diesel, and microturbine generators after a fault [16]. Another study generated a fault on a 154/22.9 kV substation modeled by the Electromagnetic Transient Program (EMTP) and examined the restoration characteristics of the system [17]. In 2012, one study examined the transient-state response of a real distribution network and the self-healing methods of the network using EMTP-Restructured Version (EMTP-RV) [18]. More recently, a 230/24 kV substation network with PV plants was modeled by EMTP Real-Time Digital Simulator (RTDS) and RSCAD [19]. A Nigerian 330 kV distribution system was modeled by DIgSILENT and the eigenvalue analysis of the system was presented in [20].

While the previous studies have focused on feeder dynamics caused by short-circuit events, some studies have examined the transient-state response to switching events of DG systems, which are not triggered by a short circuit. For example, the effect of switching events of DG systems on the IEEE 13-bus test feeder was analyzed by Fourier and wavelet transform [21]. One study also examined the islanding operation of a microgrid system after the switching events of DG systems [22]. Another study investigated the transient-state islanding operation of a distribution network that hosts fuel cells, battery systems, and a wind turbine after switching events [23].

The previous studies, however, have examined only either short-circuit events on a relatively small distribution network or transient-state responses to a switching event (which is not triggered by a short circuit). That is, Volt/Var control was not taken into account. Thus, some studies have presented various methods and algorithms on Volt/Var control in the steady state [24–28] and active power control methods [29–33]. Moreover, a transient-state active and reactive power control method of a hybrid system that consists of PV, wind, and storage systems was also modeled in [34]. However, these studies, [24–34], did not apply the active and reactive power constraints for the optimal Volt/Var control method of high-capacity DG systems upon voltage regulation. Thus, the first objective of this study is to present an optimal reactive power control method for high-capacity PV systems that takes the active and reactive power constraints into account for voltage regulation in the steady state. Moreover, none of the previous studies examined voltage variation when DG systems inject reactive power into the large distribution network with thousands of nodes in the transient state. Thus, the second objective of this study is to analyze the transient-state response of a sufficiently large actual distribution network (e.g., with thousands of or more nodes) integrated by high-capacity PV systems able to control reactive power.

This paper is organized as follows: Section 2 presents the problem statement. Section 3 describes the Volt/Var control of a DG system and the method that imports a large steady-state feeder model into DIgSILENT. Section 4 introduces case studies that verify the proposed method and discusses the simulation results. Finally, Section 5 provides the conclusions and contributions of this study.

2. Problem statement

Present regulations recommend that DG systems maintain their terminal bus voltage within 0.95 to 1.05 p.u., which corresponds to ANSI C84.1-2011 Range A, when producing power into a distribution feeder [35]. However, if either a distribution network is lightly loaded or a relatively high-capacity PV system injects power into the feeder, the system may experience an increase in overvoltage (e.g., equal or higher than 1.05 p.u.) [36]. To prevent such an overvoltage problem, the state-of-the-art inverter-based DG systems connected to the grid, particularly PV systems in this study, are able to control reactive power, which is well-known as Volt/Var control and management. However, since either clustered or scattered PV systems have continuously been connected to a large distribution network (e.g., having thousands of nodes), a study on such an overvoltage problem should take a large distribution network into account. Thus, one study examined the steady-state response of a sufficiently large distribution network (e.g., with approximately 4200 nodes) that hosts high-capacity PV systems able to control reactive power [36]. However, none of the previous studies applied the active and reactive power constraints for the optimal Volt/Var control method upon voltage regulation in the steady state. Thus, this study initially presents an optimal Volt/Var control method with the active and reactive power constraints and examines the effect of the proposed method on voltage regulation in the steady state.

The large network can be more efficiently modeled by a steady-state power-flow analysis program, or OpenDSS based on text editors, than a transient-state analysis program based on graphical editors. Furthermore, it is not feasible to draw thousands of power system components on the graphical editor. Thus, one study imported a small feeder into DIgSILENT [37]. But the study did not present the detailed method that imports feeders to DIgSILENT and verify the method for an actual large distribution feeder with PV systems. Therefore, this study proposes a method that imports the large feeder models developed in OpenDSS into a transient-state analysis program, or DIgSILENT. That is, using DIgSILENT, it develops a transient-state feeder model of a large actual distribution network with thousands of nodes. Then, high-capacity PV systems able to control Volt/Var are added to the feeder model. Thus, the model can be used for analyzing the effect of various

DG systems, including PV, either able or unable to control reactive power on an increase in overvoltage at the moment of injecting active and reactive power, which can be modeled by the following voltage droop controllers.

3. Optimal Volt/Var control

3.1. Reactive power control

The reactive power controllers can be classified by (a) constant voltage (represented by a P-V bus), (b) voltage-reactive power (*V*-*Q*) droop (represented by a Volt/Var controller), (c) voltage-reactive current droop, (d) constant reactive power (represented by a P-Q bus), (e) power factor, or (f) reactive power controllers with a function of either active power or voltage [38]. Since the *V*-*Q* droop controller is able to control the voltages of PV systems closely sited on the grid [39], it is commonly used in steady- and transient-state analyses. Fig. 1 shows the characteristics of the *V*-*Q* droop controller. For example, the controller with a droop value of 1 percent (D_i) needs an additional reactive power (Q) of 100 percent if the terminal voltage (v_i) decreases by 0.01 p.u. That is, the controller can maintain the terminal voltage to the set value by either consuming or producing reactive power. The *V*-*Q* controller is characterized by

$$\Delta V_i = V_{setpoint,i} - V_i, \tag{1}$$

$$Q_i = Q_{setpoint,i} + \Delta V_i \frac{S_{nom,i} \times 100}{D_i}. \tag{2}$$

3.2. Optimal Volt/Var control in the steady state

Eqs. (1) and (2) reveal that if the optimal droop value (D_i), that is, the line slope in Fig. 1, is known, PV systems able to either produce or consume reactive power can regulate the voltage of a bus to which PV systems are connected. Thus, one study, [27], claimed that the positive-sequence bus impedance matrix can be used to find optimal reactive power upon voltage regulation and presented the rules for constructing the bus impedance matrix of the positive-sequence network. Moreover, some studies, [27,40,41], proposed the reactive power control method. However, none of these studies used the active and reactive power constraints for the Volt/Var control method. Thus, this study proposes the following iterative Volt/Var control method.

(1) *Voltage mismatch calculation*. Let N PV systems able to control Volt/Var be connected. The proposed method calculates the deviation of the positive-sequence voltage magnitude by

$$\Delta V_i = V_{setpoint,i} - |V_{pos,i}^{(k)}|, \tag{3}$$

for $i = 1, \ldots, N$.

(2) *Calculation of current to be either injected or consumed.* It calculates the current of each phase (e.g., phases *a*, *b*, and *c*) to be injected by

$$\Delta I_{q,i,a}^{(k)} = \Delta I_{q,i,a}^{(k-1)} + \frac{1}{3}\left|\frac{\Delta V_i}{Z_{bus,i}}\right| \angle(\mathrm{Sign}(\Delta V_i) \times 90^\circ + \delta_{V,i,a}^{(k)}), \tag{4}$$

for $i = 1, \ldots, N$. Then, it adds the following active and reactive power constraints:

$$P_{min,i} = \{-pf_i \times S_{nom,i}, 0\}, \tag{5}$$

$$P_{max,i} = pf_i \times S_{nom,i}, \tag{6}$$

$$P_{PV,i}^{(k)} = \mathrm{Real}(V_i^{(k)} I_{q,i}^{(k)*}) = \begin{cases} P_{PV,i}^{(k)}, & P_{min,i} \leqslant P_{PV,i}^{(k)} \leqslant P_{max,i} \\ P_{min,i}, & P_{PV,i}^{(k)} < P_{min,i} \\ P_{max,i}, & P_{PV,i}^{(k)} > P_{max,i} \end{cases}, \tag{7}$$

$$Q_{min,i} = -\sqrt{1-pf_i^2}\, S_{nom,i}, \tag{8}$$

$$Q_{max,i} = \sqrt{1-pf_i^2}\, S_{nom,i}, \tag{9}$$

$$Q_{PV,i}^{(k)} = \mathrm{Imag}(V_i^{(k)} I_{q,i}^{(k)*}) = \begin{cases} Q_{PV,i}^{(k)}, & Q_{min,i} \leqslant Q_{PV,i}^{(k)} \leqslant Q_{max,i} \\ Q_{min,i}, & Q_{PV,i}^{(k)} < Q_{min,i} \\ Q_{max,i}, & Q_{PV,i}^{(k)} > Q_{max,i} \end{cases}, \tag{10}$$

for $i = 1, \ldots, N$. That is, if the active and reactive power outputs of PV systems exceed the limits, this study sets the active and reactive power outputs to the either minimum or maximum limits.

(3) *Convergence.* It iterates these steps (1) and (2) until the following voltage mismatch converges or all PV systems are set to their limit:

$$|\Delta V_i| \leqslant \varepsilon, \tag{11}$$

for $i = 1, \ldots, N$.In the proposed steady-state optimization method, I_q in (4) corresponds to the quadrature current related to the reactive power. The maximum power point tracking (MPPT) technique is ignored in (3)–(11). However, the MPPT technique is taken into account in the following transient-state Volt/Var control method.

3.3. Volt/Var control in the transient state

Although this study proposes the optimal Volt/Var control method of PV systems for steady-state voltage regulation, the method should be also verified in the transient state. To determine the effect of Volt/Var control on voltage regulation in the transient state, using DIgSILENT, this study models an actual substation distribution system with 4245 nodes that includes constant power, impedance, and current loads, conservation voltage regulation loads, voltage regulators, single- and three-phase transformers, capacitor banks, and PV systems with the capability of Volt/Var control. Fig. 2 shows the main controller modeled for the PV systems. The direct current (DC) voltage of the PV array (V_{dcref}) determined by the MPPT technique and the voltage of the DC link capacitor (V_{dc}) are used as input to the proportional integral (PI) controller. Then, the PI controller calculates the direct current (i_d) related to the active power. In contrast, the quadrature current (i_q) related to the reactive power is determined by the reactive power support module. In the module, if the grid voltage is maintained within a certain range of the rated voltage (e.g., ± 5 or ± 10 percent of the rated voltage), the quadrature current is set to 0 [38]. The response time of controlling the reactive current is often less than 10 s [42,43]. Moreover, inverters to voltage anomalies could respond within a clearing time of 0.16 s for $V < 0.45$ p.u. and $V \geq 1.2$ p.u., 1–11 s for 0.45 p.u. $\leq V <$ 0.6 p.u., 2 to 21 s for 0.6 p.u. $\leq V <$ 0.88 p.u., and 1–13 s for 1.1 p.u. $< V <$ 1.2 p.u. [44]. Thus, a measurement delay of 0.001 s and an MPPT delay of 5 s are used in the controller in Fig. 2. The other modules (e.g., a PV array, a DC bus, a DC link capacitor, and active power reduction and reactive power support modules) for the PV systems are presented in [38]. The detailed modeling methods and equations for the other components used in this study can be also found in [39,45,46].

Since DIgSILENT uses a graphical editor to model power system components, it is not efficient to draw each component on the graphical editor of DIgSILENT. If the system has thousands of nodes, the method may not be feasible. Thus, this study proposes to import the feeder developed in OpenDSS to DIgSILENT. For this purpose, this study

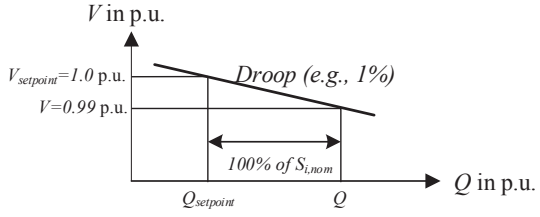

Fig. 1. Voltage-reactive power (*V*-*Q*) droop controller [39].

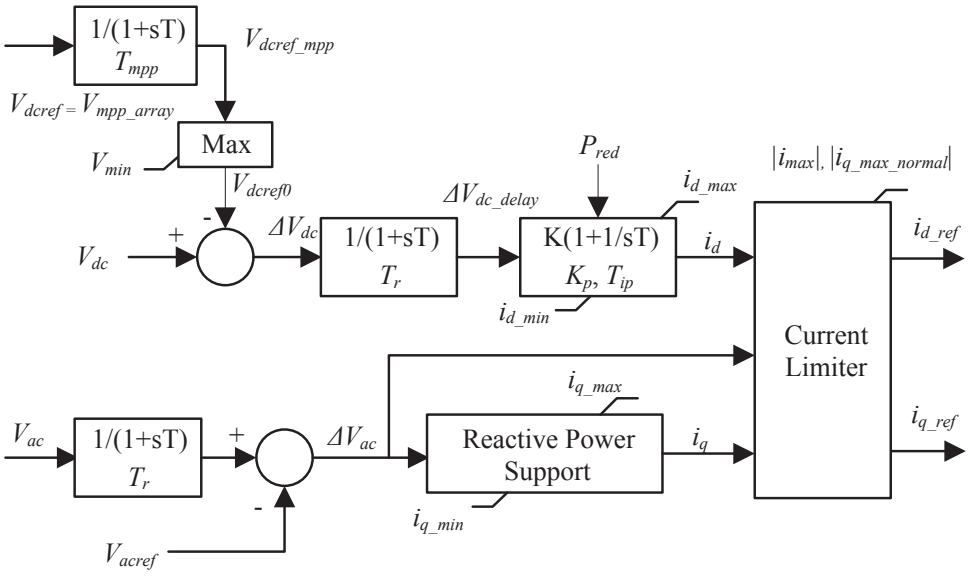

Fig. 2. The main controller model used for PV systems [38].

develops MATLAB scripts that automatically build a "DGS" file so that DIgSILENT can import from an OpenDSS feeder model. Fig. 3 illustrates the proposed interface logic of DIgSILENT that imports feeder models developed in OpenDSS through the "DGS" file interface. The MATLAB scripts are available in [47].

4. Case study

4.1. The proposed optimal Volt/Var control method in the steady state

To verify the effect of PV systems able to optimally control active and reactive power on voltage regulation, using the backward and forward sweep power-flow method [48,49], this study models the IEEE 37-bus test feeder in Fig. 4. The detailed data of the test feeder, including the voltage regulator or the on-load tap changing (OLTC) transformer, can be found in [50]. To take commonly used reactive power compensators into account, shunt capacitors with a capacity of 60 kVA, 2 percent of the feeder rating, are added to bus 701. Static var compensators (SVCs) with a capacity of 60 kVA, 2 percent of the feeder rating, are also added to bus 712. The buses (e.g., 701 and 712) are selected to minimize the losses and capacitor installation costs from an optimal capacitor placement study [51].

This study initially calculates the positive-sequence bus impedance matrix of the feeder by the four rules presented in [27]. Next, three high-capacity PV systems are connected to the optimal location of the test feeder. The optimal locations and capacities were on buses 734 (with a capacity of 22 percent of the peak power), 738 (2 percent), and 733 (1 percent) with an objective function that minimizes voltage variations and PV installation costs [27]. To take high-capacity PV systems able to optimally control active and reactive power into account, this study increases their total capacity to 50percent (e.g., on buses 734 with a capacity of 44 percent of the peak power, 738 with 4 percent, and 733 with 2 percent) in Table 1. Since the largest-capacity PV system connected to bus 734 does not violate the active and reactive power constraints (e.g., P_{max} = 1114.49 kW and Q_{max} = 539.77 kVar at a power factor [PF] of 0.9 [1]), the system successfully could regulate the bus voltage to a set voltage of 1.0 p.u. That is, the bus is maintained as a P-V bus. Fig. 5 shows the magnitudes of the voltage and current that converge to the optimal value, which can be seen as a validation of the proposed method. On the contrary, since the PV systems connected to buses 738 and 733 violate the reactive power limits (e.g., P_{max} = 101.32 kW and Q_{max} = 49.07 kVar for bus 738 and P_{max} = 50.66 kW and Q_{max} = 24.54 kVar for bus 733), the active and reactive power outputs are set to the limits while keeping a PF of 0.9 or higher [1]. That is, they are changed a P-V bus to a P-Q bus. Note that a negative power output in Table 1 indicates that PV systems inject active and reactive power to the grid.

When the electrical load varies over the time, the system could be either heavily or lightly loaded. In addition to the load, the topology of the system also changes by either opening or closing the switches, including OLTC transformers, shunt capacitors, and SVCs. Thus, this study presents the second case study with varying loads in Table 2. A heavily loaded system (e.g., a load capacity of 1.2 p.u. to the rated capacity) is initially presented. Since the system experiences an increase in undervoltage, the shunt capacitors and SVCs inject the reactive power. In contrast, the lightly loaded system (e.g., 0.4 p.u.) can experience an increase in overvoltage, so the shunt capacitors are open and the SVCs absorb the reactive power. If the load capacity to the rated capacity is in the range from 1.00 p.u. to 1.02 p.u. in Table 2, the largest-capacity PV system on bus 734 successfully could regulate the bus voltage to a set voltage of 1.0 p.u. However, if the system is lightly

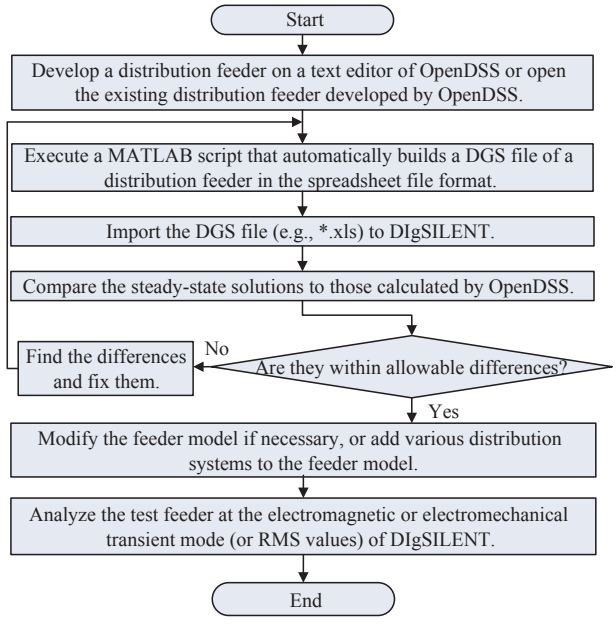

Fig. 3. The proposed method that imports a steady-state feeder model.

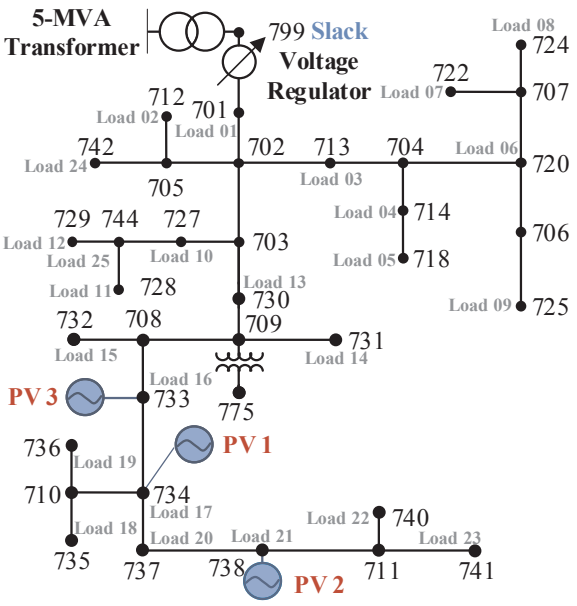

Fig. 4. The IEEE 37-bus test feeder with the three optimal PV systems [27,50].

loaded (e.g., 0.4 p.u.), the system experiences an increase in over-voltage. For example, the voltage of bus 734 is $1.0377\angle 2.01^{\circ}$ p.u. Since the largest-capacity PV system violates the reactive power limits when regulating the voltage within a set voltage of 1.0 p.u., it is changed from a P-V bus to a P-Q bus. Since the small-capacity PV systems connected to buses 738 and 733 are also kept as a P-Q bus because of the reactive power constraints.

4.2. Transient-state response of Volt/Var control

As the third case study, not only to verify the proposed method that imports a relatively large feeder but also to analyze the transient-state response of high-capacity PV systems capable of controlling reactive power, using DIgSILENT, this study models an actual substation distribution system, including feeder J1 with 4245 nodes and PV systems [52,53], in Table 3. The detailed feeder data are available in [52,53]. Fig. 6 shows the distribution system that is successfully imported to DIgSILENT and hosts the four PV systems. The distribution system has actually 13 PV systems with a total capacity of 15.3 percent to the peak power. To take high-capacity PV systems capable of controlling reactive power into account, the four largest PV systems are selected from their actual locations and their capacities are increased to 28.8 percent by doubling their actual capacity, in Table 3. In the simulations, the current PI controller with d-axis proportional gain $K_d = 1$, integration time constant $T_d = 0.01$ s, q-axis proportional gain $K_q = 1$, and integration time constant $T_q = 0.01$ s is used. The other detailed data for PV systems can be found in [38]. This study uses the electromagnetic or electromechanical (RMS values) transient mode of DIgSILENT with a version of 15.2.6 and a step size of 0.0001 s on a desktop computer (Dell XPS 8700, Intel Core i7-4770 CPU, 16 GB of memory, and a professional edition of Windows 7).

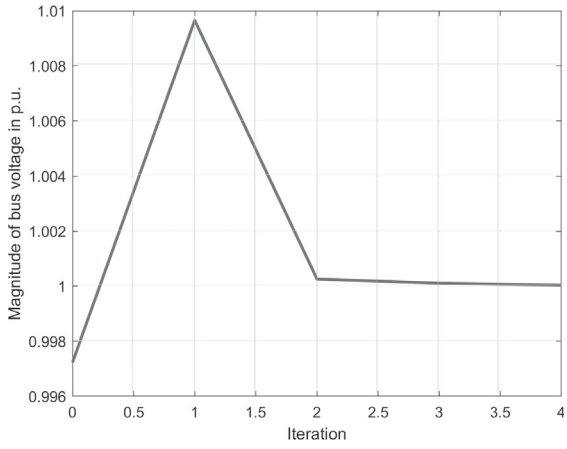

(a) Magnitude of positive-sequence voltage of bus 734

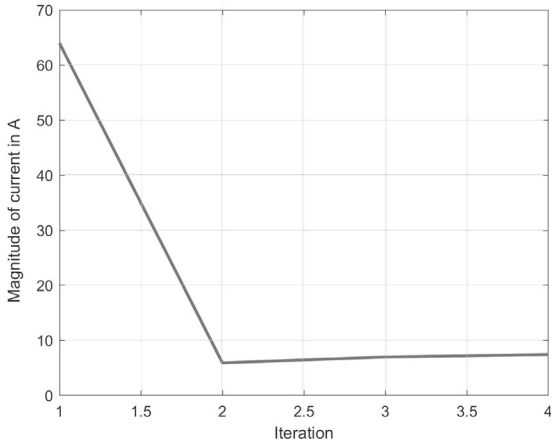

(b) Magnitude of current injected to bus 734

Fig. 5. The proposed optimal Volt/Var control method.

4.2.1. Steady-state solution comparison

This study initially compares the magnitude of the steady-state voltages to those calculated by OpenDSS. Fig. 7 presents the comparison results of the steady-state power flow of the distribution system without PV systems, calculated by both the programs, OpenDSS and DIgSILENT. The feeder models reveal a mean absolute error of 0.004768 p.u. compared to those calculated by OpenDSS [46]. The comparison can be seen as a validation of the proposed importing method. Thus, the feeder can be applied to analyze a sufficiently large test feeder with various DG systems, including PV, able to control reactive power in the transient state.

4.2.2. Transient-state response of Volt/Var control

This study has verified the effect of the optimal Volt/Var control of PV systems participating in controlling reactive power on voltage regulation in the steady state. Moreover, the steady-state analysis of a sufficiently large distribution system presented in [36] indicated that

Table 1
The voltage regulation of PV systems with the capability of optimal Volt/Var control.

Bus no.	PV		Before Volt/Var	After Volt/Var Control			
	Capacity kVA	V_{set} p.u.	Voltage p.u.	Mode –	Voltage p.u.	Current A	Power kVA
734	1238.3(44%)	1.0000	$0.9972\angle -0.32^{\circ}$	P-V	$1.0000\angle -0.13^{\circ}$	$7.43\angle -96.44^{\circ}$	$-6.79 + 61.44i$
738	112.57(4%)	1.0000	$0.9943\angle -0.34^{\circ}$	P-Q	$0.9980\angle -0.15^{\circ}$	$13.57\angle 154.01^{\circ}$	$-101.32 - 49.07i$
733	56.29(2%)	1.0000	$0.9999\angle -0.31^{\circ}$	P-Q	$1.0024\angle -0.14^{\circ}$	$6.75\angle -154.29^{\circ}$	$-50.66 + 24.54i$

Table 2
The voltage regulation of the PV systems when the load capacity varies.

Load capacity	Set voltage	Shunt capacitor	SVC	734		738		733	
				Mode	Voltage	Mode	Voltage	Mode	Voltage
1.2 p.u.	1.0 p.u.	On	Injecting	P-V	1.0001∠−0.83°	P-Q	0.9974∠−0.85°	P-Q	1.0021∠−0.74°
1.1 p.u.		On	Injecting	P-V	1.0001∠−0.49°	P-Q	0.9973∠−0.47°	P-Q	1.0022∠−0.44°
1.0 p.u.		On	Injecting	P-V	1.0000∠−0.13°	P-Q	0.9980∠−0.15°	P-Q	1.0024∠−0.14°
0.9 p.u.		Off	Absorbing	P-Q	1.0191∠1.79°	P-Q	1.0170∠1.82°	P-Q	1.0182∠1.53°
0.8 p.u.		Off	Absorbing	P-Q	1.0229∠1.84°	P-Q	1.0210∠1.87°	P-Q	1.0217∠1.58°
0.7 p.u.		Off	Absorbing	P-Q	1.0266∠1.88°	P-Q	1.0251∠1.91°	P-Q	1.0252∠1.62°
0.6 p.u.		Off	Absorbing	P-Q	1.0303∠1.92°	P-Q	1.0291∠1.95°	P-Q	1.0286∠1.66°
0.5 p.u.		Off	Absorbing	P-Q	1.0340∠1.96°	P-Q	1.0331∠2.00°	P-Q	1.0321∠1.71°
0.4 p.u.		Off	Absorbing	P-Q	1.0377∠2.01°	P-Q	1.0371∠2.04°	P-Q	1.0355∠1.75°

Table 3
The substation distribution system and PV systems modeled by DIgSILENT [36,52,53].

Substation	Total nodes	4245	
	Peak power generation	11.86 MW at 12.47 and 0.416 kV	
	Site (total length)	Northeastern area of the USA(58 miles)	
PV	Total capacity	3.42 MW (28.8% ≈ 3.42 MW/11.86 MW)	
	Name	Capacity	Bus
	PV 1	0.57 MW	X_5865228330A
	PV 2	0.38 MW	B4832_sec
	PV 3	1.52 MW	5890628219_sec,
	PV 4	0.95 MW	B51854_sec2

moderate-capacity (e.g., totally 15.3 percent of the peak power of the distribution system) and high-capacity (e.g., totally 30.6 percent of the peak power) PV systems incapable of controlling reactive power could result in a voltage rise along the feeder, even exceeding the upper limit of 1.05 p.u. In contrast, PV systems capable of controlling reactive power could alleviate the voltage rise [36]. In fact, they could present the less variation from 1.0 p.u., in other words, the better voltage regulation. However, [36] showed only the steady-state power-flow analysis. Thus, to verify the findings based on the steady-state power-flow analyses, this study models the same large distribution system in DIgSILENT using the proposed importing method. Then, four PV systems with a total capacity of 3420 kW as an example of high-capacity DG systems, which totals 28.8 percent of total peak generation of the distribution system, are added to the distribution system. It initially assumes that the grid-connected PV systems are connected at 0.5 s and start to produce their full active power while functioning as a current source. In order words, they do not participate in controlling reactive power. For example, Fig. 8(a) shows a current profile of the largest-capacity PV system with a capacity of 1.52 MW (12.8 percent of peak generation).

In Fig. 8(a), the PV system operates at a PF of unity. That is, it produces only active power. The current output of the PV system reaches 0.912 p.u. at 0.56 s. Fig. 8(b) presents a current profile of the PV system at a PF of 0.98 (leading) [54] and a droop value of 3 percent [55]. The current output of the PV system reaches 0.930 p.u. at 0.56 s.

Fig. 9(a) and (b) provide the instantaneous voltage of bus "5890628219_sec" with the largest-capacity PV system in p.u. In Fig. 9(a), the PV system produces only active power at a PF of unity. On the contrary, in Fig. 9(b), the system participates in controlling reactive power at a PF of 0.98 (leading). In the voltage outputs, the bus voltage indicates a magnitude of 1.017 p.u. before the grid-connected PV system produces its full power. The voltage output of bus "5890628219_sec" in Fig. 9(a) increases from 1.017 p.u. to 1.053 p.u. at 0.52 s, which exceeds the upper limit of 1.05 p.u. But, in Fig. 9(b), when operating at a leading PF of 0.98 with a *V-Q* droop controller, the voltage magnitude increases only to 1.030 p.u., which does not exceed 1.05 p.u.

To determine the effect of reactive power control on an increase in

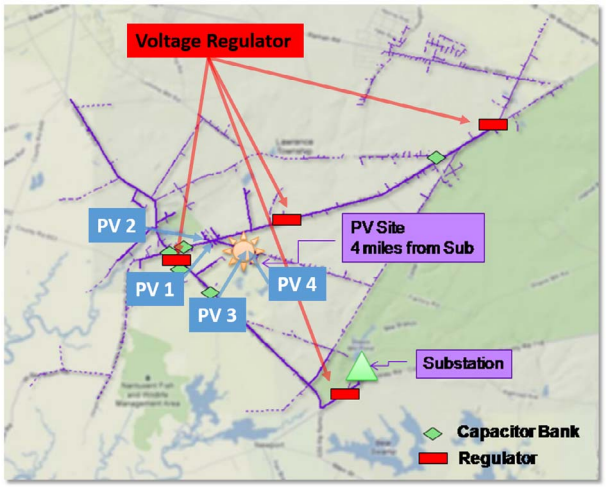

(a) Large distribution system [36, 53]

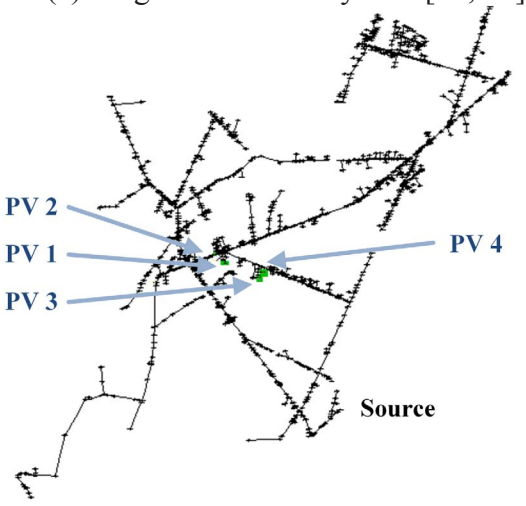

(b) The system imported to DIgSILENT

Fig. 6. The successfully developed distribution system with four PV systems in DIgSILENT.

overvoltage, this study assumes that a grid-connected PV system functions as a current source and produces its full power at a PF of unity (that is, without reactive power control) and the other case of a leading PF of 0.98 (capable of controlling reactive power with a droop value of 3 percent). Note that because (a) the PV system has a capacity of 12.8 percent of peak generation of the distribution system, which is not heavy when compared to the total capacity of the distribution system, and (b) it functions as a current source, not a voltage source, both the

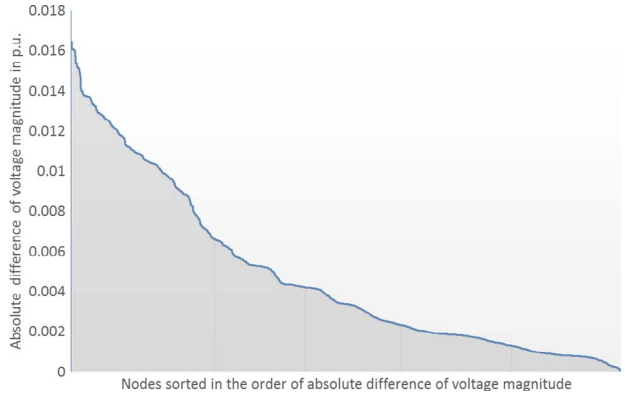

Fig. 7. The steady-state voltage magnitude differences of the substation system without PV systems for all the buses, solved by OpenDSS and DIgSILENT.

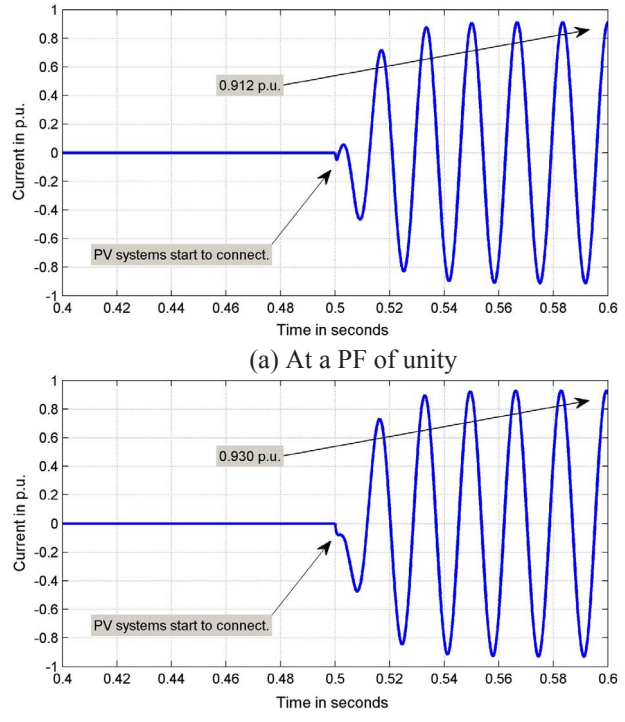

Fig. 8. Current of the largest-capacity PV system (connected to bus 5890628219_sec).

cases show the smooth and reliable integration of the PV system to the distribution system when producing its full capacity in the point of view of transient-state voltage. If PV systems increase more slowly their power or limit the output current, they can also show smoother integration to the distribution system. Expectedly, only active power injection causes an increase in overvoltage (e.g., 1.05 p.u.). On the contrary, reactive power control shows an increase of up to only 1.030 p.u. while not violating the upper limit (e.g., 1.05 p.u.). Therefore, this transient-state case study suggests that grid-connected PV systems capable of controlling reactive power can mitigate an increase in overvoltage, which is comparable to [36].

5. Conclusion

The objective of this study was to present an optimal reactive power control method with active and reactive power constraints for PV (photovoltaic) systems in the steady state. The second objective of this study is to present a method that develops the transient-state model of a sufficiently large distribution network integrated by high-capacity PV

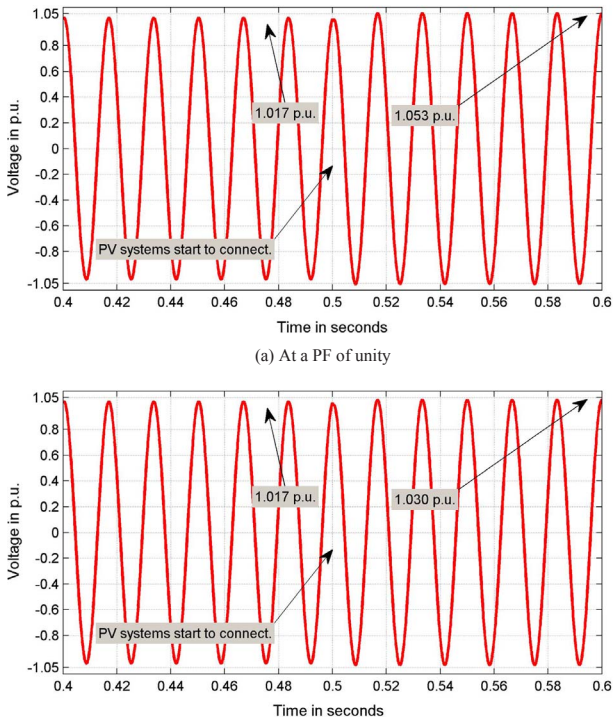

Fig. 9. Voltage of the bus with the largest-capacity PV system (12.8 percent of peak generation).

systems able to control reactive power. Using the proposed optimal Volt/Var control method, this study has showed that PV systems participating in controlling reactive power could successfully regulate the voltage of a bus to which PV systems are connected in the steady state. Then, this study has also successfully developed a transient-state feeder model of a sufficiently large actual distribution feeder using the proposed importing method. In the transient-state analysis of the distribution system, this study has found that a PV system not participating in controlling reactive power could cause an increase in overvoltage (e.g., above 1.05 p.u.) along a feeder because of the reverse power flow of the PV system. However, a *V-Q* droop controller (e.g., at a leading PF of 0.98 and a droop value of 3 percent) could mitigate an increase in overvoltage by controlling reactive power of grid-connected PV systems, which is comparable to the results of the steady-state analysis presented in [36].

The proposed optimal Volt/Var control method can be used for analyzing the effect of various DG systems such as PV, wind, microturbine, inverter-based DG systems, and other small generators able to control reactive power on voltage regulation in the steady state. Furthermore, the proposed importing method can be used for developing a transient-state model of an either small or large distribution system in DIgSILENT. Various DG systems can be added to the transient-state feeder model. Thus, they can be also used for analyzing dynamics of the feeder with various DG systems able to control Volt/Var. For example, the proposed transient-state feeder models can investigate various responses of a DG system to switching, short-circuit, or abnormal operation events in the point of view of harmonic, power-flow, and reliability analyses, which are necessary for planning, maintaining, or upgrading distribution systems integrated by DG systems.

This study has, however, not (a) applied for practical start-up procedures that utilities often use to connect PV systems into their power grids, (b) analyzed the transient-state effect of various different reactive power control (e.g., Volt/Watt or dynamic Var control) on a distribution system, and (c) implemented the MPPT technique in the steady-state voltage regulation method. But the proposed case studies can be

extended for such cases by adding small PV systems, modeling other reactive power control methods (e.g., constant voltage, voltage-reactive current droop, constant reactive power, power factor, and reactive power controllers with a function of either active power or volt), and then performing transient-state simulations as future work.

Acknowledgments

The authors gratefully acknowledge the support of the National Science Foundation, United States under Grant #1232070, which was used for part of the work presented herein. Any opinions, findings, conclusions, or recommendations expressed in this material are those of the author(s) and do not necessarily reflect the views of the National Science Foundation.

References

[1] IEEE guide for conducting distribution impact studies for distributed resource interconnection. IEEE Std 1547.7-2013; 2014. p. 1–137.
[2] Podmore R, Robinson MR. The role of simulators for smart grid development. IEEE Trans Smart Grid 2010;1(2):205–12.
[3] Watson N, Arrillaga J. Power systems electromagnetic transients simulation. IET Power Energy 2003.
[4] Yazdani A, Alizadeh O. Modelling of electronically interfaced DER systems for transient analysis. John Wiley & Sons Ltd; 2015. p. 280–316.
[5] Mahseredjian J, Dinavahi V, Martinez JA. Simulation tools for electromagnetic transients in power systems: overview and challenges. IEEE Trans Power Delivery 2009;24(3):1657–69.
[6] Hatziargyriou ND, Papadopoulos M. Transient analysis of extended distribution networks. IEEE Trans Power Delivery 1989;4(2):1290–6.
[7] Cau G, Cocco D, Petrollese M. Modeling and simulation of an isolated hybrid microgrid with hydrogen production and storage. Energy Proc 2014;45:12–21.
[8] Huang W, Zhang J, Wu Z, Niu M. Dynamic modelling and simulation of a microturbine generation system in the microgrid. In: 2008 IEEE international conference on sustainable energy technologies, Singapore, Singapore, Nov 24–27; 2008.
[9] Plet CA, Green TC. Fault response of inverter interfaced distributed generators in grid-connected applications. Electr Power Syst Res 2014;106:21–8.
[10] Darwish A, Abdel-Khalik AS, Elserougi A, Ahmed S, Massoud A. Fault current contribution scenarios for grid-connected voltage source inverter-based distributed generation with an LCL filter. Electr Power Syst Res 2013;104:93–103.
[11] Mak ST. Propagation of transients in a distribution network. IEEE Trans Power Delivery 1993;8(1):337–43.
[12] McDermit D, Shipp DD, Dionise TJ, Lorch V. Medium voltage switching transient induced potential transformer failures; prediction, measurement and practical solutions. In: 48th IEEE industrial & commercial power systems conference, Louisville, Kentucky, USA, May 20–24; 2012.
[13] Olulope PK, Folly KA, Venayagamoorthy GK. Modeling and simulation of hybrid distributed generation and its impact on transient stability of power system. In: 2013 IEEE international conference on industrial technology, Cape Town, Western Cape, South Africa, Feb. 25–28; 2013.
[14] Miao Z, Choudhry MA, Klein RL. Dynamic simulation and stability control of three-phase power distribution system with distributed generators. In: 2002 Power engineering society winter meeting, New York, NY, USA, Jan. 27–31; 2002.
[15] Thallam RS, Suryanarayanan S, Heydt GT, Ayyanar R. Impact of interconnection of distributed generation of electric distribution systems - a dynamic simulation perspective. In: 2006 Power engineering society general meeting, Montreal, Canada, June 18–22; 2006.
[16] Xyngi I, Ishchenko A, Popov M, Van der Sluis L. Transient stability analysis of a distribution network with distributed generators. IEEE Trans Power Syst 2009;24(2):1102–4.
[17] Lee BW, Rhee SB. Test requirements and performance evaluation for both resistive and inductive superconducting fault current limiters for 22.9 kV electric distribution network in Korea. IEEE Trans Appl Supercond 2010;20(3):1114–7.
[18] Spitsa V, Ran X, Salcedo R, Martinez JF, Uosef RE, de Leon F, et al. On the transient behavior of large-scale distribution networks during automatic feeder reconfiguration. IEEE Trans Smart Grid 2012;3(2):887–96.
[19] Ravindra H, Faruque MO, McLaren P, Schoder K, Steurer M, Meeker R. Impact of PV on distribution protection system. In: 2012 North American power symposium, Champaign, IL, USA, Sept 9–11; 2012.
[20] Ariyo FK, Omoigui MO. Investigation of Nigerian 330 kV electrical network with distributed generation penetration – Part I: basic analyses. Int J Energy Power Eng 2012;1(1):1–10.
[21] Vatani M. Transient analysis of switching the distributed generation units in distribution networks. Int J Appl Power Eng 2016;5(3).
[22] Katiraei F, Iravani MR. Transients of a micro-grid system with multiple distributed energy resources. In: International conference on power systems transients, Montreal, Canada, June 19–23; 2005.
[23] Voumvoulakis E, Skotinos I, Tsouchnikas A, Hatziargyriou N. Transient analysis of microgrids in grid-connected and islanded mode operation. MedPower 2004, Nicosia, Cyprus, Nov. 15–17; 2004.
[24] Thompson M, Martini T, Seeley N. Wind farm Volt/Var control using a real-time automation controller. In: 2013 Renewable energy world conference and expo North America, Orlando, Florida, USA, November 12–14; 2013.
[25] Roytelman I, Wee BK, Lugtu RL. Volt/Var control algorithm for modern distribution management system. IEEE Trans Power Syst 1995;10:1454–60.
[26] Kim I, Harley RG, Regassa R. Optimal distributed generation allocation on distribution networks at peak load and the analysis of the impact of Volt/Var control on the improvement of the voltage profile. In: 2014 North American power symposium 2014, Pullman, Washington, USA, Sept. 7–9; 2014.
[27] Kim I. Optimal distributed generation allocation for reactive power control. IET Gener Transm Distrib 2017;11(6):1549–56.
[28] de Souza BA, de Almeida AMF. Multiobjective optimization and fuzzy logic applied to planning of the Volt/Var problem in distributions systems. IEEE Trans Power Syst 2010;25:1274–81.
[29] Renedo J, García-Cerrada A, Rouco L. Active power control strategies for transient stability enhancement of AC/DC grids with VSC-HVDC multi-terminal systems. IEEE Trans Power Syst 2016;31(6):4595–604.
[30] Zhao H, Wu Q, Guo Q, Sun H, Xue Y. Optimal active power control of a wind farm equipped with energy storage system based on distributed model predictive control. IET Gener Transm Distrib 2016;10(3):669–77.
[31] Mitra A, Chatterjee D. Active power control of DFIG-based wind farm for improvement of transient stability of power systems. IEEE Trans Power Syst 2016;31(1):82–93.
[32] Stimoniaris D, Tsiamitros D, Dialynas E. Improved energy storage management and PV-active power control infrastructure and strategies for microgrids. IEEE Trans Power Syst 2016;31(1):813–20.
[33] Chen G, Lewis FL, Feng EN, Song Y. Distributed optimal active power control of multiple generation systems. IEEE Trans Ind Electron 2015;62(11):7079–90.
[34] Zhang T, Yue D, O'Grady M, O'Hare G. Transient oscillations analysis and modified control strategy for seamless mode transfer in micro-grids: a wind-PV-ES hybrid system case study. Energies 2015;8(12):13758–77.
[35] IEEE application guide for IEEE Std 1547(TM). IEEE standard for interconnecting distributed resources with electric power systems. IEEE Standard 1547.2-2008; 2009.
[36] Kim I, Harley R, Regassa R, del Valle Y. The effect of the Volt/Var control of photovoltaic systems on the time-series steady-state analysis of a distribution network. In: 2015 Power systems conference, Clemson, South Carolina, USA, March 10–13; 2015.
[37] Lin J, Zhang D, Huang J, Huang Y, Liu D. Research and development of grid model online in E imported to DIgSILENT. In: 2015 International conference on advances in mechanical engineering and industrial informatics, Zhengzhou, Henan, China, April 11–12; 2015.
[38] Kim I, Harley RG. The transient behavior of the Volt/Var control of photovoltaic systems for solar irradiation variations. In: 2016 IEEE electrical power and energy conference, Ottawa, Canada, Oct. 12–14; 2016.
[39] Weigel S. Static generator. DIgSILENT GmbH; 2010. [Tech. Rep.].
[40] Cheng CS, Shirmohammadi D. A three-phase power flow method for real-time distribution system analysis. IEEE Trans Power Syst 1995;10(2):671–9.
[41] Khushalani S, Solanki JM, Schulz NN. Development of three-phase unbalanced power flow using PV and PQ models for distributed generation and study of the impact of DG models. IEEE Trans Power Syst 2007;22(3):1019–25.
[42] Huang J, Liu M, Zhang J, Dong W, Chen Z. Analysis and field test on reactive capability of photovoltaic power plants based on clusters of inverters. J Mod Power Syst Clean Energy 2017;5(2):283–9.
[43] Ellis A, Nelson R, Von Engeln E, Walling R, MacDowell J, Casey L, et al. Reactive power performance requirements for wind and solar plants. In: 2012 IEEE Power and energy society general meeting, San Diego, CA, USA, July 22–26; 2012.
[44] IEEE standard for interconnecting distributed resources with electric power systems - amendment 1. IEEE Std 1547a-2014; 2014. p. 1–16.
[45] DIgSILENT GmbH. DIgSILENT PowerFactory reference manual. Tech. Rep.; 2015.
[46] Kim I, Regassa R, Harley R. The modeling of distribution feeders enhanced by distributed generation in DIgSILENT. In: IEEE photovoltaic specialists conference, New Orleans, LA, June 14–19; 2015.
[47] Kim I. DGS builder. Available from: < https://sourceforge.net/projects/dgs-builder/ > .
[48] Begovic MM, Kim I. Distributed renewable PV generation in urban distribution networks. In: Power systems conference and exposition, Phoenix, AZ, USA, 20–23 March; 2011.
[49] Kim I. Impact of stochastic renewable distributed generation on urban distribution networks. Ph.D. dissertation. Atlanta: Dept. Electrical and Computer Eng., Georgia Institute of Technology; 2014.
[50] Distribution Test Feeder Working Group. Distribution test feeders. Available from: < http://ewh.ieee.org/soc/pes/dsacom/testfeeders/index.html > .
[51] Subrahmanyam JBV, Radhakrishna C. A simple method for optimal capacitor placement in unbalanced radial distribution system. Electr Power Compon Syst 2010;38(11):1269–84.
[52] Electric Power Research Institute. Distributed PV monitoring and feeder analysis. Available from: < http://dpv.epri.com/ > .
[53] Electric Power Research Institute, Feeder J1. Tech. Rep.; 2014.
[54] Eaton's Cooper Power Systems. Integrated Volt/Var control, Eaton. Tech. Rep.; 2013.
[55] IEEE guide for design, operation, and integration of distributed resource island systems with electric power systems, IEEE Std 1547.4-2011, 2011.